Composition measurement in substitutionally disordered materials by atomic resolution energy dispersive X-ray spectroscopy in scanning transmission electron microscopy

Z. Chen[a], D.J. Taplin[a], M. Weyland[b,c], L.J. Allen[d], S.D. Findlay[a,*]

[a] School of Physics and Astronomy, Monash University, Clayton, Victoria 3800, Australia
[b] Monash Centre for Electron Microscopy, Monash University, Clayton, Victoria 3800, Australia
[c] Department of Materials Science and Engineering, Monash University, Clayton, Victoria 3800, Australia
[d] School of Physics, University of Melbourne, Parkville, Victoria 3010, Australia

ARTICLE INFO

ABSTRACT

The increasing use of energy dispersive X-ray spectroscopy in atomic resolution scanning transmission electron microscopy invites the question of whether its success in precision composition determination at lower magnifications can be replicated in the atomic resolution regime. In this paper, we explore, through simulation, the prospects for composition measurement via the model system of $Al_xGa_{1−x}As$, discussing the approximations used in the modelling, the variability in the signal due to changes in configuration at constant composition, and the ability to distinguish between different compositions. Results are presented in such a way that the number of X-ray counts, and thus the expected variation due to counting statistics, can be gauged for a range of operating conditions.

1. Introduction

Analytical electron microscopy via energy dispersive X-ray spectroscopy (EDX)[1] has proven to be a successful technique for exploring elemental composition in microanalysis, i.e. at sub-micron resolution [1–4]. The equation relating the number of X-ray counts N_A^{peak} in a given X-ray peak for element A to the weight concentration C_A of that element is written in various forms in the literature, but following Zaluzec [5] can be written as:

$$N_A^{peak} = [\sigma_A^{peak}(E_0)\omega_A^{peak}\Gamma_A^{peak}]\cdot\left(C_A\frac{N_0\rho t}{W_A}\right)\cdot\left(iT\varepsilon_A^{peak}\frac{\Omega}{4\pi}\right),\tag{1}$$

where $\sigma_A^{peak}(E_0)$, ω_A^{peak} and Γ_A^{peak} denote the ionization cross-section for the shell in question at accelerating voltage E_0, the fluorescence yield, and the relative transition probability of the peak[2]; C_A, W_A, N_0, ρ and t denote the weight concentration of element A, the atomic weight of element A, Avogadro's number, the sample density and sample thickness; i, T, ε_A^{peak} and Ω denote the current, the live time, the

detector efficiency for the peak being measured and the detector solid angle. Converting the measured number of X-ray counts N_A^{peak} to the sought weight concentration C_A thus requires a large number of elemental properties [terms in the first bracket in Eq. (1)], sample geometry [terms in the second bracket in Eq. (1)], and instrumental properties [terms in third bracket in Eq. (1)] to be known. This can to some extent be sidestepped by examining ratios of the measured signals:

$$\frac{C_A}{C_B} = k_{AB}^{peaks}\frac{N_A^{peak}}{N_B^{peak}},\tag{2}$$

where k_{AB}^{peaks} is the Cliff-Lorimer k-factor [6]. The current, dwell time and detector solid angle genuinely drop out in taking this ratio, but most other factors are simply subsumed (including the instrument-dependent detector efficiency, which means the Cliff–Lorimer k-factor too is instrument dependent [3]). Nevertheless, the k-factors can be determined to a good degree of precision, either from first principles calculation of the cross-sections or from measurements on samples of

---

[1] Also frequently abbreviated as XEDS or EDS.
[2] Also called the radiative partition function or relative emission rate, this describes the fraction constituted by the peak of interest to the total X-ray emission from ionization of the same shell.

known composition [1], with ∼1% sensitivity possible for the latter [4].[3]

There are various measures for the sensitivity limit in EDX. The minimum mass fraction—the smallest concentration of one element detectable in a matrix of another—was in 1980 in instruments capable of 20 nm spatial resolution estimated to be about 2 wt%, well short of the precision possible in conventional electron microprobe analysis: higher resolution means a smaller interaction volume, and a correspondingly lower X-ray generation rate if the probe electron current density is similar [1]. In 2009 and using Eq. (1), Zaluzec [5] presented an analysis of the feasibility of single atom detection by EDX. Given the tiny interaction volume implied by a single atom, other factors must increase to give a sufficient number of X-ray counts. Eq. (1) shows the most promising factors to be current, dwell time and detector solid angle. In the last decade or so, the large probe-forming convergence angles enabled by aberration-correction [7,8] and the development of brighter electron sources [9] have significantly increased the incident current. Improvements in stability [10,11] enabling registration of multiple scans [12] have increased the possible dwell time at high resolution. Larger and multiple detectors have increased the detector solid angle [13]. These gains can either improve precision at intermediate resolution EDX mapping or else can be traded-off for improvements in resolution. Atomic resolution STEM EDX imaging of crystalline samples was thereby achieved in 2010 [14–16]. Proof-of-principle single atom STEM EDX was experimentally demonstrated in 2012 [17,18].

The analysis of Zaluzec [5] implicitly assumed the single atom to be on the surface, or perhaps within a weakly scattering support. However, in many samples of interest, single atom impurities can be embedded within a crystalline matrix. In STEM annular dark field imaging, the effect of dynamical scattering of fine probes in on-axis crystals on the visibility of single atom substitutional dopants has been much explored [19–22]. That similar considerations apply for EDX may be demonstrated as follows. Consider a GaAs specimen in which a single Al atom is taken to substitutionally replace a Ga atom. Assuming 300 keV electrons incident along the [110] zone axis, an 18.4 mrad probe-forming aperture semi-angle and spatial incoherence described by convolution with a Gaussian of half-width-half-maximum 0.8 Å, Al K-peak STEM EDX images were simulated using the quantum excitation of phonons model [23], discussed further in Section 3, for different depths of the Al atom. Fig. 1(a) shows the Al K-peak EDX signal (averaged over a disk of radius 1 Å about the column) as a function of the Al dopant depth. Clear depth dependence is evident. Relative to the Al atom being at the entrance surface, the signal would be about 50% larger if the atom were at a depth of around 40 Å but around 50% smaller if it were at a depth of around 160 Å. To help explain how this comes about, Fig. 1(b) plots the electron density in the probe integrated over a disk of radius 0.3 Å about the Ga column (sufficient to encompass the effective scattering potential describing EDX) and assuming a perfectly coherent probe directly above the column. The electron density scattering along the column is clearly not uniform, but instead shows oscillatory behaviour, a process referred to loosely as "channelling".[4]

Channelling has implications for interpretation of atomic resolution STEM EDX maps. Kotula et al. [24] find *k*-factor style analysis at atomic resolution in a $Y_2Ti_2O_7$ pyrochlore is limited by the presence of a "background" signal that arises from probe scattering and spreading. Forbes et al. [25] show that, despite having the same oxygen concentration, the oxygen EDX signal on the TiO and pure O columns in $SrTiO_3$ differs due to the difference in scattering along these two
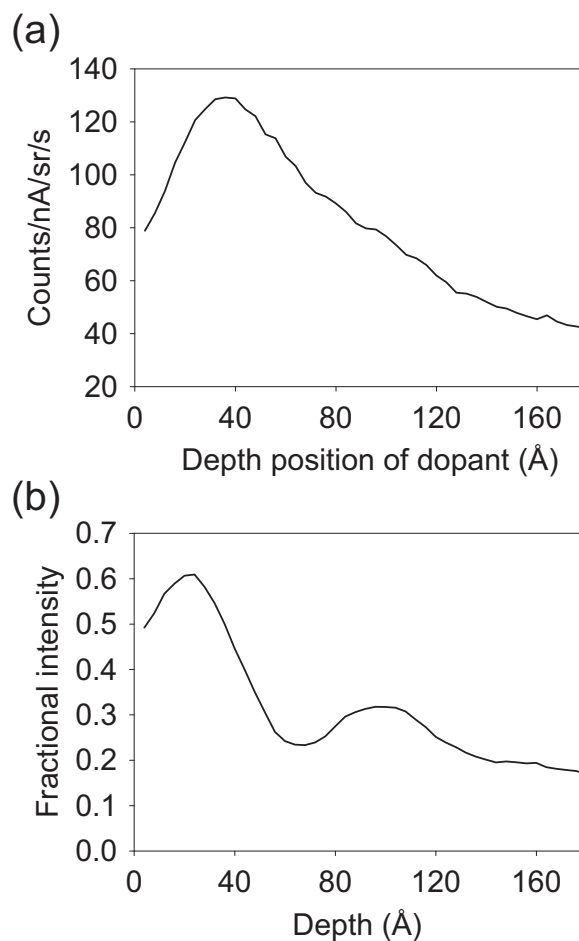

Fig. 1. (a) Depth dependence of the Al K-peak STEM EDX signal of a single Al atom in a Ga column in GaAs viewed along the [110] axis, assuming 300 keV electrons, an 18.4 mrad probe-forming aperture semi-angle, spatial incoherence described by convolution with a Gaussian of half-width-half-maximum 0.8 Å, and averaging over a disk of radius 1 Å about the column. (b) Integrated probe intensity within a disk of radius 0.3 Å around a Ga column as a function of the depth into the crystal for a coherent probe of the same accelerating voltage and probe-forming aperture semi-angle centred on the Ga column.

distinct columns. Kothleitner et al. [26] extend this to the relative distribution of signals from all elements in 2D STEM EDX images of $SrTiO_3$. Neglect of these effects for quantification in thin samples seems to show a degree of success [27–29], perhaps because integrating about columns reduces the severity of channelling effects [30], but other authors urge caution in the presence of channelling [25,31] which can become significant in samples only a few nanometers thick [32]. These complications significantly hamper the application of the *k*-factor approach to atomic resolution STEM EDX data.

To include channelling, Eq. (1) can be generalized—in a notational compromise between Ref. [5] and Refs. [32,33]—to

$$N_A^{peak}(\mathbf{R}, \Delta f) = F_A^{peak}(\mathbf{R}, \Delta f, t)\, \omega_A^{peak}\left(iT\varepsilon_A^{peak}\frac{\Omega}{4\pi}\right), \tag{3}$$

where $\mathbf{R}$ denotes the position and Δf the defocus of the STEM probe, and $F_A^{peak}(\mathbf{R}, \Delta f, t)$ gives the fraction of incident electrons causing ionization events of element *A* potentially leading to the emission of X-rays for the peak in question. Means for calculating $F_A^{peak}(\mathbf{R}, \Delta f, t)$ are well-established [34–36] and will be discussed in greater detail in Section 3. Using such simulations and a carefully characterized experiment—for which detector characterization is particularly important [37–39]—Chen et al. have shown good agreement between simulated and experimental STEM EDX signals on an absolute-scale

---

[3] For simplicity, X-ray absorption in the sample has been neglected here, though this cannot generally be done in practice. Variant approaches such as the ζ-factor method [4] may handle absorption better.

[4] The difference in shape between Figs. 1(a) and (b) results from the averaging of probe position due to disk integration and spatial incoherence in the former.